Dynamics of Regular Star Polymers: The Intrinsic Viscosity

Fabio Ganazzoli,* Giuseppe Allegra, Emanuele Colombo, and Mario De Vitis

Dipartimento di Chimica, Politecnico di Milano, via L. Mancinelli 7-20131 Milano, Italy

Received August 5, 1994; Revised Manuscript Received October 26, 1994®

ABSTRACT: The dynamics of a regular star polymer is investigated under good-solvent and Θ conditions. A self-consistent approach to the equilibrium and dynamics is proposed within the Gaussian approximation in terms of the polymer normal modes, i.e., suitable statistically-independent linear combinations of the bond vectors. The equilibrium normal modes used to study the star expansion through self-consistent free-energy minimization (see Allegra, G.; Colombo, E.; Ganazzoli, F. *Macromolecules* **1993**, *26*, 330) form a first-order approximation to the dynamical normal modes under partial-draining conditions. The latter modes are obtained by diagonalization of a matrix that depends on the intramolecular elasticity and on the hydrodynamic interaction in the preaveraging approximation, the effect of chain expansion on both being easily accounted for. If the equilibrium normal modes are used, the relaxation times, from which the intrinsic viscosity is calculated, are somewhat in error only for the collective modes describing the concerted motion of the arms, unlike those related with the independent motion of the arms; on the other hand, they yield the intrinsic viscosity to a very good approximation, thus avoiding the lengthy diagonalization. Numerical results for regular stars and linear chains are summarized by analytical equations giving the mean-square radius of gyration $\langle S^2 \rangle$, the hydrodynamic radius R_H and the intrinsic viscosity $[\eta]$. The influence of the topology is expressed through the ratios $g_Q = Q_{star}/Q_{lin}$, Q being any of the above quantities. In a good solvent, the star is only slightly more expanded than the linear chain, and so the g ratios are very close to the theoretical phantom-chain value both for $\langle S^2 \rangle$ and for R_H. Conversely, $[\eta]$ increases less in the star than in the linear chain because of the different rate of change with expansion of the intramolecular elasticity and of the hydrodynamic interaction, and so the corresponding g ratio is lower than the phantom-chain value. In the Θ state, the residual three-body interactions give a finite expansion to the star, unlike the linear chain. Therefore, we have $g_Q^{ph} \lesssim g_Q^* < g_Q^\Theta$ for $\langle S^2 \rangle$ and R_H, in agreement with experiment (the asterisk refers to the good-solvent conditions); on the other hand, we get $g_\eta^* < g_\eta^{ph} < g_\eta^\Theta$, whereas the experimental finding is $g_\eta^* < g_\eta^\Theta < g_\eta^{ph}$. The reason for this discrepancy is attributed to the preaveraging approximation, which becomes questionable for stars in the Θ state because of their large density near the branch point.

Introduction

The dynamics of a regular star polymer has been studied both theoretically and experimentally;[1−10] in particular, viscosimetry is routinely employed to investigate molecular weight and solvent effects because of its experimental simplicity. On the other hand, theoretical results were basically concerned with Θ-state phantom-chain models, either flexible,[1] or stiff,[3,4] following Zimm's method[11] within the usual preaveraging approximation for the hydrodynamic interaction. To the best of our knowledge, the only approach to the good-solvent state was attempted recently by Sammler and Schrag[5] through an approximate extension of the Zimm−Kilb phantom-chain description.[1]

A number of problems exists in improving the Zimm−Kilb description of the dynamics of phantom-chain stars, as pointed out most clearly by Douglas, Roovers, and Freed in a recent review.[2] These problems may be summarized as follows: (1) chain expansion both in a good solvent and in the Θ state (because of residual ternary interactions) modifies the normal modes; (2) the hydrodynamic interaction decreases because of coil expansion, leading to partial-draining effects; and (3) preaveraging of the hydrodynamic interaction may affect the results in a way that appears to depend on the polymer topology, according to computer simulations.[10] The interplay of these effects modifies the spectrum of relaxation times, hence the intrinsic viscosity, in a rather intricate and nonobvious way.

® Abstract published in *Advance ACS Abstracts,* January 1, 1995.

In the present paper, although still retaining the preaveraging approximation, we address points 1 and 2 above by applying to regular stars our self-consistent approach to the equilibrium and dynamics of polymers.[12] We use a coarse-grained bead-and-spring model, although retaining for simplicity the names of "atoms" and "bonds" to indicate the beads and the connecting springs. Linear and star polymers are compared through appropriate ratios of the calculated quantities, so as to bring out the effect of topology. Examples of these ratios are $g_\eta = [\eta]_{star}/[\eta]_{lin}$, $g_S = \langle S^2 \rangle_{star}/\langle S^2 \rangle_{lin}$, and $g_H = R_{H,star}/R_{H,lin}$ at the same molecular weight, where $[\eta]$ is the intrinsic viscosity, $\langle S^2 \rangle$ the mean-square radius of gyration, and R_H the hydrodynamic radius. In the good-solvent case linear and star polymers will be compared at the same value of the universal variable $\tau B\sqrt{N}$, where N is the total number of atoms, B an adimensional parameter proportional to the effective covolume per skeletal atom, and $\tau = (T - \Theta)/T$ the reduced temperature.

In order to calculate the intrinsic viscosity, we focus our attention on the spectrum of relaxation times, which are obtained from an appropriate Langevin equation expressed in terms of bond, instead of atom, coordinates.[3,4,12−15] The corresponding equation for a star polymer was first derived in general form by Guenza and Perico.[3]

Basic Equations

We consider a regular star with f arms and N total bonds, hence with N/f bonds per arm. These will be numbered sequentially from 1 to N/f starting from the branch point and we associate to each bond a vector $\mathbf{I}^{(r)}$-

0024-9297/95/2228-1076$09.00/0

(h) oriented outward, the superscript r denoting the arm number ($r = 1, 2, ..., f$). $\mathbf{R}^{(r)}(h)$ denotes the vector position of the hth atom on the rth arm, and we have $\mathbf{I}^{(r)}(h) = \mathbf{R}^{(r)}(h) - \mathbf{R}^{(r)}(h-1)$, the zeroth atom of each arm being the branch point. The bond vectors are collected in the vector array $\mathbf{L}$:

$$\mathbf{L} = [\mathbf{I}^{(1)}(1)\mathbf{I}^{(1)}(2)...\mathbf{I}^{(f)}(N/f)] \tag{1}$$

and their average scalar products define the $N \times N$ correlation matrix $\mathbf{M}$:

$$\mathbf{M} = \langle \mathbf{L}^{\mathrm{T}} \cdot \mathbf{L} \rangle \tag{2}$$

The structure of $\mathbf{M}$, which will be later of relevance, is[15]

$$\mathbf{M} = \begin{bmatrix} \mathbf{M}_0 & \mathbf{M}_1 & \cdots & \mathbf{M}_1 \\ \mathbf{M}_1 & \mathbf{M}_0 & \cdots & \mathbf{M}_1 \\ \vdots & \vdots & \ddots & \vdots \\ \mathbf{M}_1 & \mathbf{M}_1 & \cdots & \mathbf{M}_0 \end{bmatrix} \tag{3a}$$

where $\mathbf{M}_0$ and $\mathbf{M}_1$ comprise the *intra-* and *inter*arm scalar products among the bond vectors, respectively:

$$\mathrm{M}_{0,ij} = \langle \mathbf{I}^{(r)}(i) \cdot \mathbf{I}^{(r)}(j) \rangle$$

$$\mathrm{M}_{1,ij} = \langle \mathbf{I}^{(r)}(i) \cdot \mathbf{I}^{(s)}(j) \rangle \qquad r \neq s \tag{3b}$$

$\mathbf{M}$ is diagonalized by the unitary matrix $\mathbf{V}$ providing the configurational normal modes, i.e., the statistically orthogonal bond-vector combinations,[15] collected in the vector array $\tilde{\mathbf{L}}$:

$$\mathbf{V}^{*\mathrm{T}} \cdot \mathbf{M} \cdot \mathbf{V} = l^2 \gamma \text{ (diagonal)}$$

$$\tilde{\mathbf{L}} = \mathbf{L} \cdot \mathbf{V} \qquad \mathbf{V} \cdot \mathbf{V}^{*\mathrm{T}} = \mathbf{E} \tag{4}$$

$\mathbf{E}$ being the identity matrix of the appropriate order.

Due to its structure, $\mathbf{M}$ can be diagonalized in a two-step procedure by first transforming it into the block-diagonal matrix $\mathbf{M}_{\mathrm{block}}$ through the complex symmetric matrix $\mathbf{X}$ exploiting the star symmetry (see the Appendix and ref 15)

$$\mathbf{M}_{\mathrm{block}} = \mathbf{X}^* \cdot \mathbf{M} \cdot \mathbf{X} = \begin{bmatrix} \mathbf{M}_0 + (f-1)\mathbf{M}_1 & \mathbf{0} & \cdots & \mathbf{0} \\ \mathbf{0} & \mathbf{M}_0 - \mathbf{M}_1 & \cdots & \mathbf{0} \\ \vdots & \vdots & \ddots & \vdots \\ \mathbf{0} & \mathbf{0} & \cdots & \mathbf{M}_0 - \mathbf{M}_1 \end{bmatrix} \tag{5a}$$

where the $\mathbf{M}_0 - \mathbf{M}_1$ blocks repeat $(f-1)$ times. Correspondingly, the transformed vector is

$$\mathbf{L}' = \mathbf{L} \cdot \mathbf{X} \tag{5b}$$

$\mathbf{M}_{\mathrm{block}}$ is diagonalized through the block-diagonal matrix $\mathbf{W}$ formed by the submatrices $\mathbf{W}_e$ (once) and $\mathbf{W}_o$ ($f-1$ times), see eqs A-3 and A-4 in the Appendix; the e and o subscripts refer to the even and odd indices of the Fourier coordinate $q_p = \pi p/[2(N/f) + 1]$ in the trigonometric elements of $\mathbf{W}_e$ and $\mathbf{W}_o$ ($p = 2k$ or $p = 2k - 1$, see eq A-2). The nondegenerate $\mathbf{M}_0 + (f-1)\mathbf{M}_1$ block and the $(f-1)$-degenerate $\mathbf{M}_0 - \mathbf{M}_1$ block transform respectively into the diagonal matrices $l^2\boldsymbol{\alpha}$ and $l^2\boldsymbol{\beta}$ making up $l^2\gamma$ in eq 4. In conclusion, the equilibrium normal modes are given by

$$\tilde{\mathbf{L}} = \mathbf{L}' \cdot \mathbf{W} = \mathbf{L} \cdot \mathbf{X} \cdot \mathbf{W} \tag{6a}$$

so that $\mathbf{V} = \mathbf{X} \cdot \mathbf{W}$ in eq 4 and we have

$$\langle \tilde{\mathbf{L}}^{\mathrm{T}} \cdot \tilde{\mathbf{L}} \rangle = l^2 \gamma = l^2 \begin{bmatrix} \boldsymbol{\alpha} & & & \\ & \boldsymbol{\beta} & & \\ & & \ddots & \\ & & & \boldsymbol{\beta} \end{bmatrix} \tag{6b}$$

The elements of $\boldsymbol{\alpha}$ and $\boldsymbol{\beta}$, α_k^2 and β_k^2, $k = 1, 2, ..., N/f$, are the strain ratios of the mean-square amplitudes of the normal modes. For the bead-and-spring polymer with no correlation among the bond vectors, $\mathbf{M}/l^2$ reduces to the unit matrix, and so does γ. Conversely, the elements α_k^2 and β_k^2 are larger than unity in case of chain expansion with respect to the phantom chain, and smaller in case of contraction. Note that the collective modes have a small k index, whereas the local modes have a large k index.

Knowledge of the normal modes $\tilde{\mathbf{L}}$ and of their mean-square strain ratios α_k^2 and β_k^2 allows the calculations of the mean-square interatomic distances $\langle r_{ij}^2 \rangle$ between atoms i and j on arms r and s, respectively:[15]

$$\langle r_{ij}^2 \rangle_{rs} = \frac{l^2}{f} \sum_{k=1}^{N/f} \{(a_{ij}^{(k)})^2 \alpha_k^2 + [(f-1)(b_{ij}^{(k)})^2 + 2f(1 - \delta_{rs}) b_{0i}^{(k)} b_{0j}^{(k)}] \beta_k^2\} \tag{7a}$$

where (see also eq A-2 for q_p and C):

$$a_{ij}^{(k)} = C \sin[q_{2k}(h+j)/2] \sin[q_{2k}(h-j)/2] / \sin(q_{2k}/2)$$

$$b_{ij}^{(k)} = C \cos[q_{2k-1}(h+j)/2] \sin[q_{2k-1}(h-j)/2] / \sin(q_{2k-1}/2) \tag{7b}$$

The mean-square radius of gyration $\langle S^2 \rangle$ and the hydrodynamic radius R_{H} are given by

$$\langle S^2 \rangle = [2(N+1)^2]^{-1} \sum_{i,j} \langle r_{ij}^2 \rangle \tag{8a}$$

$$R_{\mathrm{H}}^{-1} = (N+1)^{-2} \sum_{i,j} \langle r_{ij}^{-1} \rangle \qquad (i \neq j) \tag{8b}$$

where the double sums run over all the star atoms. Note that $\langle S^2 \rangle$ can also be written as a single sum over the normal modes through eqs 7a,b.

Numerical values of α_k^2 and β_k^2 were recently obtained by us from self-consistent free-energy minimization both in the case of good-solvent expansion[15] and of Θ-state expansion[16] (see later) and they will be used as such in the following.

Within the generalized Gaussian approximation, $\mathbf{M}$ entirely determines the elastic forces acting on the chain atoms,[3,14,17] and the Langevin equation is[3,14]

$$-3k_{\mathrm{B}}T\, \mathbf{L} \cdot \mathbf{M}^{-1} \cdot \mathbf{B} - \zeta \frac{\partial}{\partial t} \mathbf{L} = \mathbf{Y} \tag{9}$$

ζ being the atomic friction coefficient, $\mathbf{Y}$ the random Brownian force and

$$\mathbf{B} = \mathbf{a}\mathbf{H}\mathbf{a}^{\mathrm{T}} \tag{10}$$

In turn, $\mathbf{H}$ is the preaveraged $(N+1) \times (N+1)$ hydrodynamic interaction matrix

$$H_{ij} = \delta_{ij} + \frac{\zeta}{6\pi\eta_S l}\left\langle\frac{l}{r_{ij}}\right\rangle(1 - \delta_{ij}) \tag{11}$$

where η_S is the solvent viscosity and the reciprocal averages are approximated through the Gaussian expression

$$\langle r_{ij}^{-1}\rangle = \left(\frac{6}{\pi\langle r_{ij}^2\rangle}\right)^{1/2} \tag{12}$$

a is the rectangular $N \times (N + 1)$ connectivity matrix transforming the array of the atomic coordinates **R** into that of the bond vectors **L**:

$$\mathbf{a} = \left[\begin{array}{c|cccc} \mathbf{a}_0 & \mathbf{a}_1 & \mathbf{0} & \cdots & \mathbf{0} \\ \mathbf{a}_0 & \mathbf{0} & \mathbf{a}_1 & \cdots & \mathbf{0} \\ \vdots & \vdots & \vdots & \ddots & \vdots \\ \mathbf{a}_0 & \mathbf{0} & \mathbf{0} & \cdots & \mathbf{a}_1 \end{array}\right] \tag{13}$$

where the column vector $\mathbf{a}_0$ and the $(N/f) \times (N/f)$ matrix $\mathbf{a}_1$ are

$$\mathbf{a}_0 = \begin{bmatrix} -1 \\ 0 \\ 0 \\ \vdots \\ 0 \end{bmatrix} \qquad \mathbf{a}_1 = \begin{bmatrix} 1 & 0 & 0 & \cdots & 0 \\ -1 & 1 & 0 & \cdots & 0 \\ 0 & -1 & 1 & \cdots & 0 \\ \vdots & \vdots & \vdots & \ddots & \vdots \\ 0 & 0 & 0 & -1 & 1 \end{bmatrix} \tag{14}$$

In order to decouple the equations making up the matrix equation 9, we switch to normal coordinates[3,4,11,13,17] by diagonalizing the product $\mathbf{M}^{-1}\mathbf{B}$. We first employ the two-step procedure used in the diagonalization of **M** through the matrix $\mathbf{V} = \mathbf{X}\cdot\mathbf{W}$, since this is the appropriate matrix for the phantom chain in the free-draining approximation.[14] Afterward, we seek to improve it by a further step in the partial-draining case considered here. Let us note that $\mathbf{B} = \mathbf{aHa}^T$ has the same structure as the equilibrium correlation matrix **M** (see eq A-5); the blocks $\mathbf{B}_0$ on the main diagonal and $\mathbf{B}_1$ outside it comprise the hydrodynamic interaction among atoms within the same arm or belonging to two different arms. Postmultiplying eq 9 by **X** and remembering eqs 5a,b, we get

$$-\sigma l^2\mathbf{L}'\mathbf{M}_{\text{block}}^{-1}\mathbf{D}_{\text{block}} - \frac{\partial}{\partial t}\mathbf{L}' = \mathbf{Y}' \tag{15}$$

where $\mathbf{Y}'$ is a transformed Brownian velocity ($\mathbf{Y}' = \zeta^{-1}\mathbf{Y}\cdot\mathbf{X}$), $\sigma = (3k_BT)/(\zeta l^2)$ is the bond rate constant and $\mathbf{D}_{\text{block}} = \mathbf{X}^*\cdot\mathbf{B}\cdot\mathbf{X}$ is the block-diagonal matrix analogous to $\mathbf{M}_{\text{block}}$.

In the free-draining approximation,[14] **H** reduces to the unit matrix and $\mathbf{B} = \mathbf{aa}^T$ is diagonalized by **V** or, equivalently, $\mathbf{D}_{\text{block}}$ is diagonalized by the same matrix as $\mathbf{M}_{\text{block}}$, that is, by **W**, in the case of the phantom chain. This diagonalization is not guaranteed in the presence of the hydrodynamic interaction, but, in analogy to what is found for the linear chain,[11] $\mathbf{D} = \mathbf{W}^T\cdot\mathbf{D}_{\text{block}}\cdot\mathbf{W}$ is expected to be almost diagonal. Therefore, by applying the **W** transformation to eq 15 we have

$$-\sigma\tilde{\mathbf{L}}\gamma^{-1}\mathbf{D} - \frac{\partial}{\partial t}\tilde{\mathbf{L}} = \mathbf{Y}'' \tag{16}$$

where γ^{-1} and $\tilde{\mathbf{L}}$ are given by eqs 6a,b and $\mathbf{Y}''$ is a new transformed Brownian velocity. The block structure of $\gamma^{-1}\mathbf{D}$ is reported in the Appendix (see eq A-8). Note that the equilibrium expansion of the polymer *affects both the elastic force per normal mode* through γ^{-1} *and the strength of the hydrodynamic interaction* through **D**, hence through **H** (see eqs 11, 12, and 7).

The *dynamical* normal modes, collected in the vector array $\mathcal{L}$, and the spectrum of relaxation times are obtained by diagonalization of $\gamma^{-1}\mathbf{D}$ through the **Z** matrix:

$$\mathbf{Z}^{-1}(\gamma^{-1}\mathbf{D})\mathbf{Z} = (\sigma\boldsymbol{\tau})^{-1} \qquad \text{(diagonal)}$$

$$\mathcal{L} = \tilde{\mathbf{L}}\cdot\mathbf{Z} \tag{17a}$$

$\boldsymbol{\tau}^{-1}$ and **Z** have the same block structure as γ^{-1} (or γ for that matter) and **W**:

$$\boldsymbol{\tau}^{-1} = \begin{bmatrix} \boldsymbol{\tau}_e^{-1} & & & \\ & \boldsymbol{\tau}_o^{-1} & & \\ & & \ddots & \\ & & & \boldsymbol{\tau}_o^{-1} \end{bmatrix} \qquad \mathbf{Z} = \begin{bmatrix} \mathbf{Z}_e & & & \\ & \mathbf{Z}_o & & \\ & & \ddots & \\ & & & \mathbf{Z}_o \end{bmatrix} \tag{17b}$$

Therefore, we can split the eigenvalue problem of eq 17 involving an $N \times N$ matrix in two eigenvalue problems involving $(N/f) \times (N/f)$ matrices, corresponding to the even modes of unit multiplicity and to the odd modes of multiplicity $(f - 1)$. The eigenvalue equations are

$$\mathbf{Z}_e^{-1}\boldsymbol{\alpha}^{-1}\mathbf{D}_e\mathbf{Z}_e = (\sigma\boldsymbol{\tau}_e)^{-1} \qquad \text{even modes} \tag{18a}$$

$$\mathbf{Z}_o^{-1}\boldsymbol{\beta}^{-1}\mathbf{D}_o\mathbf{Z}_o = (\sigma\boldsymbol{\tau}_o)^{-1} \qquad \text{odd modes} \tag{18b}$$

where $\mathbf{D}_e$ and $\mathbf{D}_o$ are the blocks making up **D** (see also eq A-8).

Finally, the relaxation times of the even modes are given by the elements $\tau_{e,k}$ and of the odd modes by the element $\tau_{o,k}$ of the above matrices ($k = 1, 2, \ldots, N/f$). The dynamical normal modes can be expressed in terms of the bond vectors array **L** as

$$\mathcal{L} = \mathbf{L}\cdot(\mathbf{V}\cdot\mathbf{Z}) \tag{19}$$

The Langevin equation is now decoupled and can be solved through standard procedures,[12,17] the dynamic averages of interest may then be calculated in a straightforward way.

In the following we focus our attention on the hydrodynamic radius and on the intrinsic viscosity, which depends only on the spectrum of the relaxation times:[1]

$$[\eta] = \frac{N_{Av}k_BT}{2M\eta_s}\left[\sum_{k=1}^{N/f}\tau_{e,k} + (f-1)\sum_{k=1}^{N/f}\tau_{o,k}\right] \tag{20}$$

where M is the molar mass and N_{Av} is Avogadro's constant.

Numerical Calculations

The diagonalization of $\boldsymbol{\alpha}^{-1}\mathbf{D}_e$ and of $\boldsymbol{\beta}^{-1}\mathbf{D}_o$ was performed numerically, as anticipated; the strain ratios α_k^2 and β_k^2 (i.e., the elements of the diagonal matrices $\boldsymbol{\alpha}$ and $\boldsymbol{\beta}$) were taken from our previous results in tabular form both for good-solvent[15] and for Θ-solvent[16] expansion. The reduced friction coefficient per chain atom, $\zeta/6\pi\eta_S l$, was set equal to 0.25 in agreement with current estimates.[3,12,13,18] As said in the preceding section, the matrices $\boldsymbol{\alpha}^{-1}\mathbf{D}_e$ and of $\boldsymbol{\beta}^{-1}\mathbf{D}_o$ are almost diagonal; in either case the off-diagonal terms are nonnegligible compared to those on the main diagonal only for the

most collective modes (i.e., the modes with a low k index). Therefore, in order to save computer time we diagonalized the 25 × 25 upper-left blocks only, keeping otherwise the diagonal terms with larger mode indices. We checked that this entailed a negligible error on the relaxation times throughout the computations. Although the eigenvalue eqs 18a,b involve diagonalization of two nonsymmetrical matrices, the eigenvalues, i.e., the elements of $\boldsymbol{\tau}^{-1}$, are always real.

The Zimm–Hearst approximation,[11,19] consisting of retaining only the diagonal terms of $\boldsymbol{\alpha}^{-1}\mathbf{D}_e$ and $\boldsymbol{\beta}^{-1}\mathbf{D}_o$, slightly underestimates the relaxation times of the most collective modes, but is entirely adequate for more localized modes, and so the intrinsic viscosity is affected to an even smaller extent (see eq 20). Bloomfield and Zimm[20] showed that the error entailed by this approximate procedure is very small for the linear phantom chain. However, this result has a general validity, at least if one is concerned with the intrinsic viscosity: the relative error in $[\eta]$ is about the same for linear and branched chains in any solvent condition, being anyway less than 2%.

The Phantom Chain

This is the familiar bead-and-spring chain already considered by Zimm and Kilb,[1] forming our reference model. It is recovered in the present formalism by setting $\alpha_k^2 \equiv \beta_k^2 \equiv 1$, whence the interatomic mean-square distances are given by $\langle r_{ij}^2 \rangle = l^2|i-j|$ for atoms on the same arm and by $\langle r_{ij}^2 \rangle = l^2(i+j)$ for atoms on different arms. The relaxation times of the $(f-1)$-times degenerate odd modes are independent from f, since these modes have a node at the branch point[1] and therefore contribute to the noncorrelated motion of the arms. Conversely, the even modes have no such node and contribute to the concerted motion of the arms. The corresponding relaxation times are thus affected by the arm number, somewhat increasing with f for a given mode index, and the errors entailed by the Zimm–Hearst approximation[11,19] may become rather serious. As an example, the relaxation time of the first odd mode (showing by far the largest error) is underestimated by less than 2%, whereas for the first even mode the error amounts to about 1.3% for $f = 2$, and up to 33% for $f = 18$. On the other hand, the odd modes dominate for stars, the more so the larger is f, due to the different multiplicities (see eq 20), and the intrinsic viscosity is affected only slightly. *The same relative errors also apply to the good-solvent case*, where the full numerical procedure is more lengthy, thus supporting the general validity of the Zimm–Hearst approximation. In other words, even in the presence of the hydrodynamic interaction the free-draining normal modes yield the correct intrinsic viscosity to a very good approximation in any solvent condition. However, in the following we shall report for completeness the results obtained with the full procedure.

The intrinsic viscosity of the phantom polymers is proportional to $N^{1/2}$ in the long-chain limit, whereas plots of $[\eta]_{ph}/\sqrt{N}$ are linear with $N^{-1/2}$ due to the finite size of the molecules. Therefore, the topological ratio $g_\eta^{ph} = [\eta]_{ph,star}/[\eta]_{ph,lin}$ displays some weak molecular weight dependence. At large N the best-fit linear regression may be written as

$$g_\eta^{ph} = g_{\eta,\infty}^{ph}(1 + a_f/\sqrt{N}) \tag{21a}$$

$g_{\eta,\infty}^{ph}$ and a_f being reported in Table 1. Within numerical errors, the asymptotic values are equal to those obtained by Zimm and Kilb:[1] in fact, in the limit $N \to \infty$ the hydrodynamic partial draining considered here coincides with the impermeable-coil, or Zimm, limit[11] used in ref 1. Therefore, $g_{\eta,\infty}^{ph}$ is also given to within 1% by the approximate expression of Zimm and Kilb[1] *employing only the sums* $\sum_k \tau_{e,k}$ and $\sum_k \tau_{o,k}$ *pertaining to the linear chain*:

$$g_{\eta,\infty}^{ph} \cong \left(\frac{2}{f}\right)^{3/2}[0.334 + (f-1)0.666] \tag{22}$$

$[\eta]_{ph,star}$ may be eventually obtained through $g_{\eta,\infty}^{ph}$ and $[\eta]_{ph,lin}$, where (see also ref 11)

$$[\eta]_{ph,lin} = (2.84 \times 10^{23})l^3\sqrt{N/M_0} \tag{21b}$$

Here, M_0 is the molar mass per chain atom and the mean-square length l^2 may be written as $C_\infty l^2$, C_∞ being the characteristic ratio and l the chemical bond length.

Similar results apply to the hydrodynamic radius: $R_{H,ph}$ is asymptotically proportional to $N^{1/2}$, while for finite chains we find a linear relationship between $R_{H,ph}/\sqrt{N}$ and $N^{-1/2}$. Correspondingly, the topological ratio $g_H = R_{H,star}/R_{H,lin}$ follows an equation similar to eq 21a. Within numerical accuracy, related to the extrapolation to $N^{-1/2} \to 0$, $g_{H,\infty}^{ph}$ is given by[21]

$$g_{H,\infty}^{ph} = \frac{f^{1/2}}{2 - f + \sqrt{2}(f-1)} \tag{23a}$$

Again, for the phantom polymer $R_{H,star}$ is obtained from this equation and the relationship[12]

$$R_{H,lin} = \frac{3}{8}\left(\frac{\pi N}{6}\right)^{1/2} l \tag{23b}$$

Table 1. The Intrinsic-Viscosity Phantom Polymer and Θ Polymer Topological Ratio $g_{\eta,\infty}$ and the Coefficient a_f for Different Values of f (See Eq 21), and the Topological Ratio of the Hydrodynamic Radius $g_{H,\infty}$ for the Θ Star (for the Phantom Polymer see Eq 23)

	phantom		Θ		
f	$g_{\eta,\infty}^{ph}$	a_f	$g_{\eta,\infty}^{\Theta}$	a_f	$g_{H,\infty}^{\Theta}$
6	0.6955	+0.0177	0.7197	−0.2655	0.8081
12	0.5149	−0.0606	0.5855	−1.5086	0.6636
18	0.4272	−0.1316	0.5514	−3.3256	0.5971

Good-Solvent Expansion

The calculations were carried out for the linear chain and the 6-arm star having $N/f = 200$ in order to use previous numerical results[15] of α_k^2 and β_k^2. In ref 15, we showed that the equilibrium "normal" modes of eq 6 are not strictly orthogonal under large expansion; however, they produce off-diagonal elements in the $\boldsymbol{\alpha}$ and $\boldsymbol{\beta}$ matrices that are smaller than the diagonal ones by at least 1 order of magnitude in the worst case (i.e., the most collective modes of the 6-arm star under large expansion). *A fortiori*, their effect on the mean-square interatomic distances and radius of gyration is even smaller, so that they can be neglected to a very good approximation. Accordingly, here we shall use only the diagonal terms of $\boldsymbol{\alpha}$ and $\boldsymbol{\beta}$ obtained with the full procedure of ref 15.

In comparison with the phantom-chain model, the effect of chain expansion is 2-fold: (1) the elastic force in the dynamic equation decreases, due to the greater correlation among bond vectors (the elements of $\mathbf{M}$ are

larger, see eqs 3); (2) the hydrodynamic interaction becomes weaker due to the larger interatomic separation ($\langle r_{ij}^{-1}\rangle$ decreases upon chain expansion, hence the elements of **H** become smaller, see eq 11). In the dynamic eq 16, factor 1 translates into smaller values of the elements of the diagonal matrix γ^{-1} and factor 2 into smaller values of the elements of the quasi-diagonal matrix **D**. As a result, the relaxation times increase with chain expansion compared to the phantom-chain values, the more so the smaller the mode index k is (i.e., the more collective is the mode). The increase of $\tau_{e,k}$ and $\tau_{o,k}$ is mostly due to the increasing strain ratios α_k^2 and β_k^2, respectively, while the hydrodynamic interaction undergoes a relatively minor change, since it depends only on the reciprocal averages $\langle r_{ij}^{-1}\rangle$.

A first result concerning the diagonalization of $\alpha^{-1}\mathbf{D}_e$ and of $\boldsymbol{\beta}^{-1}\mathbf{D}_o$ (eq 18) is worthy of comment. As anticipated, the Zimm–Hearst approximation underestimates the relaxation times, hence $[\eta]$, roughly by the same amount as with the phantom chain, both for the linear polymer and the 6-arm star (about 2% for $[\eta]$). As a consequence, for both architectures the α_η^3 ratio, defined as

$$\alpha_\eta^3 = \frac{[\eta]}{[\eta]_{ph}} \tag{24}$$

is unaffected to within 0.2% by this approximation compared to the full procedure. The same conclusion applies to the topological ratio $g_\eta^* = [\eta]_{star}/[\eta]_{lin}$, the star superscript denoting the good-solvent state.

For a given arm length ($N/f = 200$ in our case) and a given reduced temperature $\tau = (T - \Theta)/T$, the 6-arm star shows a larger α_η^3 than the linear chain; this is due to the larger number of repulsive interactions because of the larger *total* number of atoms. Conversely, the star structure has two contrasting effects: on the one hand, it produces a larger density near the star core, which enhances the overall expansion; on the other, it provides a topological constraint at the branch point opposing such expansion and leading to a loss of correlation *across the branch point*.[15] As a result, the star expansion is highly nonaffine, being concentrated near the branch point *within each arm*. Therefore, it turns out that the linear and the star polymer have very similar expansion factors $\alpha_S^2 = \langle S^2\rangle/\langle S^2\rangle_{ph}$, with $\alpha_{S,star}^2 \gtrsim \alpha_{S,lin}^2$, as a function of the universal variable $z = \tau B\sqrt{N}$. For later reference, the plots of α_S^2 vs z obtained in ref 15 can be well approximated in the range $z \leq 2$ with the analytical expressions

$$\alpha_{S,lin}^2 = [1 + 9.571z + 17.8z^2 + 79.3z^3]^{2/15} \qquad f = 2 \text{ (linear)} \tag{25a}$$

$$\alpha_{S,star}^2 = [1 + 10.866z + 14.4z^2 + 98.9z^3]^{2/15} \qquad f = 6 \text{ (star)} \tag{25b}$$

The coefficients of the terms linear with z within square brackets yield the exact first-order perturbative results,[22] whereas the exponent gives asymptotically $\langle S^2\rangle \propto N^{2\nu}$, with the Flory exponent $2\nu = 6/5$. In both cases the largest relative error of the analytical fit to the numerical results is about 1% for $z \approx 1$, being otherwise quite smaller. These equations show that, for a given z, the 6-arm star is slightly more expanded than the linear chain throughout the good-solvent regime. The topological ratio g_S is expressed as

$$g_S^* = \frac{\langle S^2\rangle_{star}}{\langle S^2\rangle_{lin}} = g_S^{ph}\frac{\alpha_{S,star}^2}{\alpha_{S,lin}^2} \tag{26a}$$

where[23]

$$g_S^{ph} = \frac{3f - 2}{f^2} \tag{26b}$$

Due to the inequality $\alpha_{S,star}^2 > \alpha_{S,lin}^2$, we have $g_S^* > g_S^{ph}$ throughout the range $z > 0$, with the asymptotic value $g_S^* = 1.03 g_S^{ph}$ for $z \to \infty$. This result is in good agreement with renormalization group calculations and with experiment (see ref 2 and references therein).

For the same reason as discussed for α_S^2, plots of α_η^3 vs $z = \tau B\sqrt{N}$ for the linear and the 6-arm star are again rather close to one another (see Figure 1); however, $\alpha_{\eta,star}^3$ is marginally larger than $\alpha_{\eta,lin}^3$ at intermediate z, then becomes somewhat smaller at larger z. (Note incidentally that, since in a good solvent $z = \tau B\sqrt{N}$ is the universal variable uniquely determining the strain ratios α_k^2 and β_k^2, it is also the universal variable for α_η^3 in the present approach.) The numerical results are well approximated by analytical expressions analogous to those in eqs 25:

$$\alpha_{\eta,lin}^3 = [1 + 3.291z + 2.912z^2]^{3/10} \qquad f = 2 \text{ (linear)} \tag{27a}$$

$$\alpha_{\eta,star}^3 = [1 + 3.616z + 2.351z^2]^{3/10} \qquad f = 6 \text{ (star)} \tag{27b}$$

where the exponents outside the square brackets yield the asymptotic relationship $[\eta] \propto N^{4/5}$. The perturbative results cannot be well reproduced because of the use of the Gaussian approximation for $\langle r_{ij}^{-1}\rangle$, as also found in a previous work;[24] therefore, we chose to fit the results at larger z only ($z \geq 0.5$) in order to extrapolate more confidently to $z \to \infty$; the fitting error was anyway less than 0.5% throughout the z range shown in Figure 1. Equations 27 show that $\alpha_{\eta,star}^3$ is larger than $\alpha_{\eta,lin}^3$ at small z, whereas the opposite is true at large z. As a result, proceeding in analogy with g_S^*, and writing

$$g_\eta^* = \frac{[\eta]_{star}}{[\eta]_{lin}} = g_\eta^{ph}\frac{\alpha_{\eta,star}^3}{\alpha_{\eta,lin}^3} \tag{28}$$

we have for g_η^* a small increase over g_η^{ph} at a small expansion (small z), but a pronounced decrease at larger z. This behavior is due to a subtle interplay of the rate of change with z of the elastic force and of the hydrodynamic interaction in the linear vs the star polymer.

Figure 2 reports the plot of g_η^* as a function of z calculated with the interpolating eqs 27a,b and g_η^{ph} of the previous section. (The number of atoms is large enough that the difference between g_η^{ph} and $g_{\eta,\infty}^{ph}$ is utterly negligible.) The solid line indicates the range of z over which eqs 27 were fitted, whereas the dotted curve is extrapolated. The asymptotic value for the 6-arm star levels off at a value equal to $0.938 g_\eta^{ph}$. This decrease with respect to g_η^{ph} is in semiquantitative agreement with experimental results, which show some scatter of g_η^* in the range comprised between 5 to 10% below the Θ value, apparently depending on the poly-

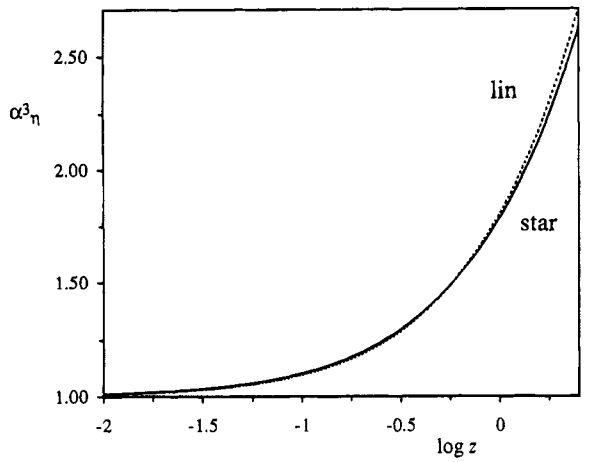

Figure 1. The expansion ratio $\alpha_\eta^3 = [\eta]/[\eta]_{ph}$ of the linear chain and of the 6-arm star in a good solvent plotted as a function of the universal variable $z = \tau B\sqrt{N}$ giving the strength of the excluded volume (see text).

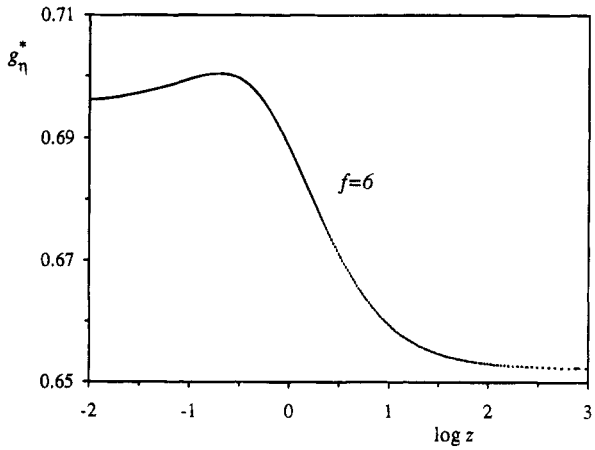

Figure 2. The topological ratio $g_\eta^* = [\eta]_{star}/[\eta]_{lin}$ for the 6-arm star in a good solvent as a function of z (see also Figure 1). The solid curve indicates the range of z wherein the numerical calculations were actually performed and the dotted curve the extrapolated results obtained with eqs 27 and 28 and $g_\eta^{ph} = 0.6955$ (see text and Table 1).

mer. In particular, g_η^* appears to be somewhat larger for polyisoprene[6] than for polystyrene,[7] hence closer to, although smaller than, the experimental g_η^Θ.

Conversely, the hydrodynamic radius follows the same expression pattern as the radius of gyration. Thus, the calculated expansion ratio over the phantom-chain value, $\alpha_H = R_H/R_{H,ph}$ may be written as

$$\alpha_{H,lin} = [1 + 3.91z + 3.80z^2]^{1/10} \qquad f = 2 \text{ (linear)} \quad (29a)$$

$$\alpha_{H,star} = [1 + 4.68z + 6.51z^2]^{1/10} \qquad f = 6 \text{ (star)} \quad (29b)$$

which again does not reproduce accurately the perturbative results. The hydrodynamic radius is determined by the reciprocal averages $\langle r_{ij}^{-1}\rangle$ only and follows the same pattern as the radius of gyration, with $\alpha_{H,star} > \alpha_{H,lin}$ throughout the good-solvent regime. As a consequence, the topological ratio g_H^*, defined by

$$g_H^* = \frac{R_{H,star}}{R_{H,lin}} = g_H^{ph}\frac{\alpha_{H,star}}{\alpha_{H,lin}} \quad (30)$$

is always larger than g_H^{ph} with an asymptotic value $g_H^* = 1.055g_H^{ph}$ for $z \to \infty$, a result in reasonable agreement with experimental values (see ref 2 and references therein). The larger increase of the topological g ratio of the *linear* quantity R_H compared to that of the (*quadratic*) quantity $\langle S^2\rangle$ is related to the larger expansion of short strands close to the branch point which affects the former dimension to a much larger extent.

As a conclusion of this section, we note that the calculated plot of g_η^* is qualitatively similar to that of the ring polymer:[24] in fact, like the star, the ring has a larger intramolecular density than the linear chain due to topological constraints. Incidentally, the results for the intrinsic viscosity of the ring are qualitatively consistent both with exact perturbative results (not available for stars, to the best of our knowledge) and with experimental data and renormalization group results at large expansion.[24]

The Θ State

The Θ state is experimentally attained at the temperature at which the second virial coefficient vanishes, that is, when the molecules are noninteracting in pairs. Since the repulsive three-body interactions between two molecules must be compensated for by temperature-dependent two-body attractions, it turns out that in a star polymer the Θ temperature must be lower than in a linear chain, even more so the larger is f and/or the smaller is N/f.[25-27] In fact, because of its topology, the star has a larger multiplicity of three-body repulsions between two molecules than a linear chain. However, if the molar mass is very large, the region close to the branch point has a negligible effect and a universal asymptotic Θ temperature is reached.[25-27]

This compensation of two- and three-body *inter*molecular interactions brings about an analogous compensation of the corresponding *intra*molecular interactions within the linear chain, but not within a star. In the latter, three-body repulsions among three atoms *on three different arms* are inherently noncompensated by two-body attractions, since no intermolecular counterpart exists.[16] To put it differently, the most important three-body repulsions arise among relatively close atoms; if two of the three atoms belong to the same arm, they can be included into a single renormalized "atom" in a coarser grained description, and the interaction reduces to an effective two-body interaction. No such renormalization is possible if the three atoms belong to three different arms. As a result, the star has a finite expansion with respect to the phantom chain, unlike the linear chain, and g_S^Θ is larger than both g_S^{ph} and g_S^*. Furthermore, it is not a universal ratio since it depends on the three-body interaction parameter. These theoretical results are in good agreement with experiment.[16]

Turning to the intrinsic viscosity, the qualitative arguments put forward at the beginning of the previous section hold again: the Θ expansion of the star, although finite and much smaller than in a good solvent, makes $\alpha_k^2, \beta_k^2 \geq 1$, the equality sign holding for all but the most collective modes, and so $\langle r_{ij}^{-1}\rangle \leq \langle r_{ij}^{-1}\rangle_{ph}$. Therefore, in the Θ state the relaxation times of the star, hence the intrinsic viscosity, must be larger than in the phantom chain. The molar-mass dependence of $[\eta]_{star}$ is similar to that of the phantom chain, hence of g_η^Θ as well (see eq 21); $g_{\eta,\infty}^\Theta$ and a_f for this case are reported in Table 1 and indeed $g_\eta^\Theta > g_\eta^{ph}$ (remember that the linear chain in the Θ state is well described by the phantom

chain). However, this theoretical prediction is ruled out by experiment, since g_η^Θ is invariably found to be *smaller* than the calculated value $g_{\eta,}^{ph}$ unlike the corresponding g_S values. According to that discussed above, whatever the analytical details, this result is somewhat puzzling.

Let us point out in this context that the hydrodynamic radius R_H does show the expected behavior, unlike the intrinsic viscosity.[2,8,9] Because of the residual three-body expansion of the star, we must have the same trend as calculated for the mean-square radius of gyration, namely $g_H^\Theta > g_H^{ph}$. (Table 1 reports the values for the Θ state in the $N \to \infty$ limit, while those for the phantom chain are given by eq 23.) In full generality, this inequality should therefore hold for all the topological ratios discussed here. This is in agreement with experiment for $\langle S^2 \rangle$ and, qualitatively, for R_H, but not for $[\eta]$. The most likely explanation put forward for the latter discrepancy resides in the treatment of the hydrodynamic interaction, in particular the preaveraging approximation. Freire *et al.*,[10] following earlier suggestions by Zimm[28,29] and Fixman,[30] used computer simulations to generate instantaneous conformations wherefrom appropriate averages are obtained with non-preaveraged hydrodynamic interaction. In this way, they showed that the preaveraging approximation *overestimates* the intrinsic viscosity by an amount which depends both on the solvent quality and on the star functionality.[10] The relative error amounts to about 10% for linear chains and to 47% for 12-arm stars in a good solvent, but rises respectively to 25% and to 90% in the Θ state, roughly reflecting the density increase near the branch point. Therefore, the errors entailed by preaveraging may be quite serious in the case of the intrinsic viscosity for polymers with locally large densities of atoms for topological reasons. If we applied these corrective factors to our results of Table 1, they would be in reasonable agreement with experiment, whereas the phantom-chain results would become too small. Conversely, similar computer simulations suggest that the hydrodynamic radius is *underestimated* by a smaller amount weakly dependent on the number of arms;[29] however, the errors are not large enough to alter qualitatively the results.

On the other hand, the possibility of some concentration-dependent intramolecular screening within stars is effectively ruled out by experiment, since it *decreases* the off-diagonal terms within the **H** matrix (see eq 11), thus *increasing* the relaxation times, hence the intrinsic viscosity and the calculated g_η^Θ ratio.

Concluding Remarks

A self-consistent theory of the equilibrium and dynamics of star polymers in dilute solution is proposed. We employ in either case a normal mode description of the molecule. The *equilibrium* modes are obtained from diagonalization of the matrix **M** formed through the scalar products among the bond vectors.[12,15] These normal modes allow an easy (numerical) calculation of the interatomic distances, hence of the radius of gyration and of the hydrodynamic radius, and provide the *dynamical* normal modes in the free-draining limit.[14] In turn, these form a first-order approximation to the *true* dynamical normal modes under partial-draining conditions. In the present paper, the spectrum of relaxation times, hence the intrinsic viscosity, is calculated from equilibrium results obtained in previous papers for different solvent conditions, namely good-solvent[15] and Θ-solvent[16] conditions. The effect of chain expansion on the elastic potential and on the hydrodynamic interaction is accounted for and the correct normal modes are obtained by numerical diagonalization of the matrix embodying them ($\gamma^{-1}\mathbf{D}$ in eq 17) *formed through the equilibrium normal modes*. The relaxation times of the modes describing the concerted motion of the arms are somewhat increased by the diagonalization compared to the diagonal terms of $\gamma^{-1}\mathbf{D}$, even more so with a larger number of arms. However, this increase is negligible for the modes describing the independent motion of the arms, which are the most important because of their larger multiplicity. As a result, the intrinsic viscosity is not greatly affected by the complete procedure, thus lending support to the so-called Zimm–Hearst approximation of using the free-draining normal modes *insofar as the intrinsic viscosity is required*.

The approach was applied to the linear chain and the 6-arm star in a good solvent. The results obtained in ref 15 (equilibrium properties) and in the present paper (dynamical properties) are expressed through the expansion factors of the mean-square radius of gyration, of the intrinsic viscosity and of the hydrodynamic radius, with respect to the corresponding theoretical phantom polymer. The numerical values are summarized by the analytical expressions of eqs 25, 27, and 29, which form the basic results. Using these equations together with eqs 26, 28, and 30, and the g values of the phantom chains (see eqs 26b and 23 and Table 1) we get the topological g ratios between the corresponding properties of the star and of the linear polymer, for a given molecular weight.

In the good-solvent regime, the star expansion is mostly concentrated *within* the arms, and both the mean-square radius of gyration $\langle S^2 \rangle$ and the hydrodynamic radius R_H increase (with respect to the hypothetical phantom-chain model) slightly more than in the linear chain (eqs 25 and 29). Therefore, the corresponding g ratios are very close to, but always larger than, the phantom-chain values. Conversely, the interplay between the rate of change of the elastic potential and of the hydrodynamic interaction is more subtle and the relative increase of the intrinsic viscosity may be either larger or smaller in the star than in the linear chain, depending on the expansion regime (see eqs 27a,b and Figure 1). As a result, the topological ratio $g_\eta^* = [\eta]_{star}/[\eta]_{lin}$ is close to the phantom-chain value (see Table 1 and Figure 2), being slightly larger in the vicinity of Θ (i.e., in the perturbative range), but somewhat smaller by a few percent in the asymptotic good-solvent region. In this case, the preaveraging approximation has a minor effect, since we are considering a relatively lightly branched star ($f = 6$) in a good solvent, therefore without a large density near the branch point. Conversely, in the Θ state the residual three-body repulsions surviving within the star increase both $\langle S^2 \rangle$ and R_H compared with the phantom chain, unlike the linear chain where such interactions are effectively missing; this should lead to a larger g_η^Θ ratio. This prediction is not borne out by experiment, the preaveraging approximation being the major source of the observed discrepancy. However, this approximation is much less severe for the hydrodynamic radius, so as not to alter qualitatively our results. To sum up, we predict the inequalities $g_Q^{ph} \lesssim g_Q^* < g_Q^\Theta$, the Q subscript being either S or H (i.e., relating to $\langle S^2 \rangle$ and to R_H). These results are in agreement with experiment, unlike the corresponding viscosimetric ratios: our

results indicate $g_\eta^* < g_\eta^{ph} < g_\eta^\Theta$, whereas the experimental finding is $g_\eta^* < g_\eta^\Theta < g_\eta^{ph}$. Interestingly, Douglas and Freed[2,31] showed that the *dominant* excluded-volume contribution to $\langle S^2 \rangle$ and to R_H is expressed by topology-independent functions (eq 2.4 of ref 2), which therefore cancel out when forming the corresponding g_Q^* ratios. Thus, the latter depend only very weakly on excluded volume and are very close to g_Q^{ph}.

Among the theoretical approaches to the dynamics of star polymers going beyond the pioneering work by Zimm and Kilb,[1] we mention those by Guenza *et al.*,[3,4] who included the effect of chain stiffness through the use of a suitable freely rotating model, but otherwise adopted a phantom-chain model in that long-range interactions were neglected. They first adopted[4] a partially stretched model with a larger stiffness in the central part of the star due to the local density. Alternatively, they considered[3] a star whose flexibility at the branch point increases with an increasing arm number. Being concerned with the local dynamics, they focussed their interest on the spectrum of relaxation times, from which they got, for example, the bond relaxation times, measured in NMR experiments.

A different approach was adopted by Sammler and Schrag,[5] who took into account the effect of chain expansion on the hydrodynamic interaction either through simple scaling relationships or from previous renormalization results to evaluate the reciprocal averages $\langle r_{ij}^{-1} \rangle$. However, they entirely neglected the effect of chain expansion on the elastic potential. In terms of our dynamic eq 9, they accounted for the decrease upon good-solvent expansion of the hydrodynamic interaction in the **B** matrix, but not for the corresponding change in $\mathbf{M}^{-1}$, which yields the elastic potential. Their results appear therefore questionable for this approximation.

In these treatments, as well as in our approach, the hydrodynamic interaction was included in the preaveraging approximation, which is somewhat in error even for the linear chain, in particular for the intrinsic viscosity. In the star, this error increases with the arm number, but in good solvent it is still similar to that of the linear chain up to about 6 arms, so that it largely cancels out when the appropriate topological ratios are taken. On the other hand, the hydrodynamic radius is much less affected by preaveraging, and in a way that does not qualitatively alter the results.

Acknowledgment. This work was financially supported by the Italian Ministry of University and of Scientific and Technological Research (MURST, 40%) and of the Italian Research Council (CNR, Progetto Finalizzato Chimica Fine e Secondaria).

Appendix

The correlation matrix **M** in eq 3 is reduced to the block-diagonal form $\mathbf{M}_{block}$ through the matrix **X** (see eq 5), where ($\varphi = 2\pi/f$)

$$\mathbf{X} = f^{-1/2} \begin{bmatrix} \mathbf{E} & \mathbf{E} & \mathbf{E} & \cdots & \mathbf{E} \\ \mathbf{E} & \mathbf{E}e^{i\varphi} & \mathbf{E}e^{i2\varphi} & \cdots & \mathbf{E}e^{i(f-1)\varphi} \\ \mathbf{E} & \mathbf{E}e^{i2\varphi} & \mathbf{E}e^{i4\varphi} & \cdots & \mathbf{E}e^{i2(f-1)\varphi} \\ \vdots & \vdots & \vdots & \ddots & \vdots \\ \mathbf{E} & \mathbf{E}e^{i(f-1)\varphi} & \mathbf{E}e^{i2(f-1)\varphi} & \cdots & \mathbf{E}e^{i(f-1)^2\varphi} \end{bmatrix} \tag{A-1}$$

The second step in the diagonalization of **M** involves a transformation of $\mathbf{M}_0 + (f-1)\mathbf{M}_1$ and $\mathbf{M}_0 - \mathbf{M}_1$ (see eq 5) through the matrices $\mathbf{W}_e$ and $\mathbf{W}_o$, respectively with elements ($N/f \gg 1$)

$$W_{e,hk} = C \sin[(h - 1 + 1/f)q_{2k}]$$

$$W_{o,hk} = C \cos[(h - {}^1/_2)q_{2k-1}]$$

$$C = \frac{2}{\left(2\frac{N}{f} + 1\right)^{1/2}}$$

$$q_p = \frac{\pi p}{2\frac{N}{f} + 1} \tag{A-2}$$

In the above, the e and o subscripts stand for for the even and odd values of the p index of the Fourier coordinate q_p, a small p corresponding to collective modes, and a large p to local modes. Sending the interested reader to ref 15 for more details, we write

$$\mathbf{W}_e^T \cdot [\mathbf{M}_0 + (f-1)\mathbf{M}_1] \cdot \mathbf{W}_e = l^2 \boldsymbol{\alpha}$$

$$\mathbf{W}_o^T \cdot [\mathbf{M}_0 - \mathbf{M}_1] \cdot \mathbf{W}_o = l^2 \boldsymbol{\beta} \tag{A-3}$$

$\boldsymbol{\alpha}$ and $\boldsymbol{\beta}$ being diagonal matrices denoted in the text as strain ratios of the normal modes. In the phantom chain they reduce to the identity matrix of order $N/f \times N/f$. The matrix **V** (see eqs 4 and 6) is given by

$$\mathbf{V} = \mathbf{X} \cdot \mathbf{W} = \mathbf{X} \cdot \begin{bmatrix} \mathbf{W}_e & & & \\ & \mathbf{W}_o & & \\ & & \ddots & \\ & & & \mathbf{W}_o \end{bmatrix} \tag{A-4}$$

As for the dynamic eq 9, after some tedious algebra, we have, from eqs 11, 13, and 14

$$\mathbf{B} = \mathbf{a}\mathbf{H}\mathbf{a}^T = \begin{bmatrix} \mathbf{B}_0 & \mathbf{B}_1 & \cdots & \mathbf{B}_1 \\ \mathbf{B}_1 & \mathbf{B}_0 & \cdots & \mathbf{B}_1 \\ \vdots & \vdots & \ddots & \vdots \\ \mathbf{B}_1 & \mathbf{B}_1 & \cdots & \mathbf{B}_0 \end{bmatrix} \tag{A-5}$$

where the $(N/f) \times (N/f)$ matrices $\mathbf{B}_0$ and $\mathbf{B}_1$ comprise the intra- and interarm contributions, respectively, the branch point entering both matrices. They can be expressed as the sum of a free-draining term and of a hydrodynamic interaction term as follows:

$$\mathbf{B}_0 = \mathbf{B}_0^{fd} + \frac{\zeta}{6\pi\eta_S l} \mathbf{B}_0^{hi} \tag{A-6a}$$

$$\mathbf{B}_1 = \mathbf{B}_1^{fd} + \frac{\zeta}{6\pi\eta_S l} \mathbf{B}_1^{hi} \tag{A-6b}$$

where the free-draining matrices are given by

$$\mathbf{B}_0^{fd} = \begin{bmatrix} 2 & -1 & 0 & \cdots & 0 \\ -1 & 2 & -1 & \cdots & 0 \\ 0 & -1 & 2 & \cdots & 0 \\ \vdots & \vdots & \vdots & \ddots & -1 \\ 0 & 0 & 0 & -1 & 2 \end{bmatrix}$$

$$\mathbf{B}_1^{fd} = \begin{bmatrix} 1 & 0 & \cdots & 0 \\ 0 & 0 & \cdots & 0 \\ \vdots & \vdots & \ddots & \vdots \\ 0 & 0 & 0 & 0 \end{bmatrix} \quad \text{(A-7a)}$$

and the hydrodynamic-interaction matrices by

$$(\mathbf{B}_0^{hi})_{ij} = \left\langle \frac{l}{r_{ij}} \right\rangle_{11} + \left\langle \frac{l}{r_{i-1j-1}} \right\rangle_{11} - \left\langle \frac{l}{r_{i-1j}} \right\rangle_{11} - \left\langle \frac{l}{r_{ij-1}} \right\rangle_{11}$$

$$(\mathbf{B}_1^{hi})_{ij} = \left\langle \frac{l}{r_{ij}} \right\rangle_{12} + \left\langle \frac{l}{r_{i-1j-1}} \right\rangle_{12} - \left\langle \frac{l}{r_{i-1j}} \right\rangle_{12} - \left\langle \frac{l}{r_{ij-1}} \right\rangle_{12} \quad \text{(A-7b)}$$

(The 11 and 12 subscripts refer to atoms on the same or on different arms, respectively.)

B is first transformed in the block-diagonal form $\mathbf{D}_{block}$ (see eq 15) through the matrix **X**, and then into the quasidiagonal matrix **D** through the matrix **W**, in analogy to that done above for **M**. The structure of $\gamma^{-1}\mathbf{D}$ (see eq 16) is therefore

$$\gamma^{-1}\mathbf{D} = \begin{bmatrix} \alpha^{-1}\mathbf{D}_e & \mathbf{0} & \cdots & \mathbf{0} \\ \mathbf{0} & \beta^{-1}\mathbf{D}_o & \cdots & \mathbf{0} \\ \vdots & \vdots & \ddots & \vdots \\ \mathbf{0} & \mathbf{0} & \cdots & \beta^{-1}\mathbf{D}_o \end{bmatrix} \quad \text{(A-8a)}$$

where we defined

$$\alpha^{-1}\mathbf{D}_e = \alpha^{-1}\mathbf{W}_e{}^T\cdot[\mathbf{B}_0 + (f-1)\mathbf{B}_1]\cdot\mathbf{W}_e$$

$$\beta^{-1}\mathbf{D}_o = \beta^{-1}\mathbf{W}_o{}^T\cdot[\mathbf{B}_0 - \mathbf{B}_1]\cdot\mathbf{W}_o \quad \text{(A-8b)}$$

It may be seen from these expressions that the matrices to be diagonalized are nonsymmetrical; furthermore, eqs A-6 show that the relaxation rates (see eqs 18) can be expressed as the sum of a free-draining part and of a hydrodynamic interaction part.

References and Notes

(1) Zimm, B. H.; Kilb, R. W. *J. Polym. Sci.* **1959**, *37*, 19.
(2) Douglas, J. F.; Roovers, J.; Freed, K. F. *Macromolecules* **1990**, *23*, 4168.
(3) Guenza, M.; Perico, A. *Macromolecules* **1992**, *25*, 5942.
(4) Guenza, M.; Mormino, M.; Perico, A. *Macromolecules* **1991**, *24*, 6168.
(5) Sammler, R. L.; Schrag, J. L. *Macromolecules* **1989**, *22*, 3435.
(6) Hadjichristidis, N.; Roovers, J. *J. Polym. Sci., Polym. Phys. Ed.* **1974**, *12*, 2521.
(7) Roovers, J.; Bywater, S. *Macromolecules* **1974**, *7*, 443.
(8) Roovers, J.; Hadjichristidis, N.; Fetters, L. J. *Macromolecules* **1983**, *16*, 214.
(9) Huber, K.; Burchard, W.; Fetters, L. J. *Macromolecules* **1984**, *17*, 541.
(10) Freire, J. J.; Rey, A.; Bishop, M.; Clarke, J. H. R. *Macromolecules* **1991**, *24*, 6494.
(11) Zimm, B. H. *J. Chem. Phys.* **1956**, *24*, 269.
(12) See, e.g.: Allegra, G.; Ganazzoli, F. *Adv. Chem. Phys.* **1989**, *75*, 265.
(13) Perico, A. *Acc. Chem. Res.* **1989**, *22*, 336.
(14) Raos, G.; Allegra, G.; Ganazzoli, F. *J. Chem. Phys.* **1994**, *100*, 7804.
(15) Allegra, G.; Colombo, E.; Ganazzoli, F. *Macromolecules* **1993**, *26*, 330.
(16) Ganazzoli, F. *Macromolecules* **1992**, *25*, 7357.
(17) Perico, A.; Ganazzoli, F.; Allegra, G. *J. Chem. Phys.* **1987**, *87*, 3677.
(18) Allegra, G.; Higgins, J. S.; Ganazzoli, F.; Lucchelli, E.; Brückner, S. *Macromolecules* **1984**, *17*, 1253.
(19) Hearst, J. E. *J. Chem. Phys.* **1962**, *37*, 2547.
(20) Bloomfield, V.; Zimm, B. H. *J. Chem. Phys.* **1966**, *44*, 315.
(21) Stockmayer, W. H.; Fixman, M. *Ann. N. Y. Acad. Sci.* **1953**, *57*, 334.
(22) Yamakawa, H. *Modern theory of polymer solutions*; Harper & Row: New York, 1971; Chapter III, Section 17a.
(23) Zimm, B. H.; Stockmayer, W. H. *J. Chem. Phys.* **1949**, *17*, 1301.
(24) Ganazzoli, F.; Fontelos, M. A. *Polymer* **1988**, *29*, 1648.
(25) Ganazzoli, F.; Allegra, G. *Macromolecules* **1990**, *23*, 262.
(26) Allegra, G.; Ganazzoli, F. *Prog. Polym. Sci.* **1991**, *16*, 463.
(27) Cherayil, B. J.; Douglas, J. F.; Freed, K. F. *J. Chem. Phys.* **1987**, *87*, 3089.
(28) Zimm, B. H. *Macromolecules* **1980**, *13*, 592.
(29) Zimm, B. H. *Macromolecules* **1984**, *17*, 795.
(30) Fixman, M. *J. Chem. Phys.* **1983**, *78*, 1588.
(31) Douglas, J. F.; Freed, K. F. *Macromolecules* **1984**, *17*, 2344; **1985**, *18*, 201.

MA9410983